Ondřej Winter; Petr Sváček

Numerical simulation of flow induced airfoil vibrations with large amplitudes

Persistent URL: `http://dml.cz/dmlcz/703065`

NUMERICAL SIMULATION OF FLOW INDUCED AIRFOIL VIBRATIONS WITH LARGE AMPLITUDES

Ondřej Winter, Petr Sváček

Department of Technical Mathematics, Faculty of Mechanical Engineering,
Center of Advanced Aerospace Technology, Czech Technical University in Prague,
Karlovo náměstí 13, Praha 2, Česká republika
ondrej.winter@fs.cvut.cz, petr.svacek@fs.cvut.cz

Abstract: This paper is interested with the numerical simulation of the fluid-structure interaction problem realized with the aid of the OpenFOAM package. The case of flow past oscillating NACA 0012 profile was chosen. The loose, strong and combined strong coupling algorithms were tested. The results are presented and a significant improvement of the combined coupling algorithm is shown.

Keywords: finite volume method, OpenFOAM, aeroelasticity, arbitrary lagrangian eulerian method

MSC: 76M12,74F10

1. Introduction

The presented paper is concerned with the numerical simulation of the two-dimensional viscous incompressible flow past a moving airfoil, which is considered as a solid flexibly supported body with two degrees of freedom, allowing its vertical and torsional oscillations. This problem was addressed previously in e.g. [3], [10], [13]. The same problem was studied in [7] where the results of the turbulent incompressible flow model were compared to the solution of the laminar flow model. The results showed that the turbulence is necessary to take into account in aeroelastic computations even for low speeds (and low Mach number) air flows. In reality the transition from laminar to turbulent flow exists on the surface of the airfoil. We adopted a model based on the non-turbulent fluctuations proposed by Walters and Cokljat [11] referred to as k-k_L-ω model.

The main attention is paid to the fluid-structure coupling algorithms. Particularly, the pressure implicit with splitting of operators (PISO) and semi-implicit method for pressure linked equations (SIMPLE) algorithms are used, see e.g.[3], [8]. A combination of PISO and SIMPLE algorithms is called PIMPLE, see [6]. Fluid

flow solver is coupled with the structure using both the loose and the strong coupling algorithms. Realization of the numerical experiments is done with the aid of the open-source software OpenFOAM, see [12]. PIMPLE based solver *pimpleDyMFoam* is modified and coupled with the rigid body motion library *sixDoFRigidBodyMotion*. The method is applied on a test case and numerical results are shown.

2. Mathematical model

In this section, the formulation of the initial-boundary value problem describing the interaction of the fluid flow with the moving airfoil is presented. In order to enable the computations on the moving domain, the governing equations are formulated in the arbitrary Lagrangian-Eulerian (ALE) form, see [10]. The viscous incompressible turbulent flow in computational domain $\Omega_t \subset \mathbb{R}^2$ for any $t \in (0, T)$ is described by the Reynolds-averaged Navier-Stokes (RANS) equations (see e.g. [4], [9]) in the ALE conservative form (see e.g. [13])

$$\frac{1}{J}\frac{D^{\mathcal{A}}(J\boldsymbol{v})}{Dt} + \mathrm{div}[\boldsymbol{v} \otimes (\boldsymbol{v} - \boldsymbol{w})] = -\mathrm{grad}(p) + \mathrm{div}(\mathsf{T} + \mathsf{R})/\rho, \tag{1}$$

$$\mathrm{div}(\boldsymbol{v}) = 0,$$

where $\boldsymbol{v}$ is the mean velocity vector, p is the mean kinematic pressure, i.e., the mean pressure divided by the constant fluid density ρ, T is the mean viscous stress tensor and R is the Reynolds stress tensor. Symbol $\boldsymbol{w}$ denotes the so-called ALE velocity, symbol J denotes the Jacobian of the ALE mapping and symbol $D^{\mathcal{A}}(\cdot)/Dt$ represents the ALE derivative, see e.g. [10]. The components of the viscous stress tensor T are for a Newtonian fluid given by

$$\mathsf{T}_{ij} = \mu\left(\frac{\partial v_i}{\partial x_j} + \frac{\partial v_j}{\partial x_i}\right), \tag{2}$$

where $\mu = \rho\nu$ is the dynamic viscosity, ν is the kinematic viscosity. The Reynolds stress tensor R is approximated using the turbulent viscosity approach, see e.g. [5], [9], i.e,

$$\mathsf{R}_{ij} = 2\rho\nu_T\left(\frac{\partial v_i}{\partial x_j} + \frac{\partial v_j}{\partial x_i} - \frac{1}{3}\frac{\partial v_k}{\partial x_k}\delta_{ij}\right) - \frac{1}{3}\rho k\delta_{ij}. \tag{3}$$

Here, ν_T is the turbulent kinematic viscosity and k is the total kinetic energy of fluctuations. The turbulent kinematic viscosity ν_T and the total kinetic energy of fluctuations k need to be further specified by the turbulence model. The k-k_L-ω model is used, which consists of three transport equations. The equation for the laminar kinetic energy k_L written in ALE form reads

$$\frac{1}{J}\frac{D^{\mathcal{A}}(Jk_L)}{Dt} + \mathrm{div}[k_L(\boldsymbol{v} - \boldsymbol{w})] = P_{k_L} - R_{BP} - R_{NAT} - D_L + \mathrm{div}[\nu\,\mathrm{grad}(k_L)], \tag{4}$$
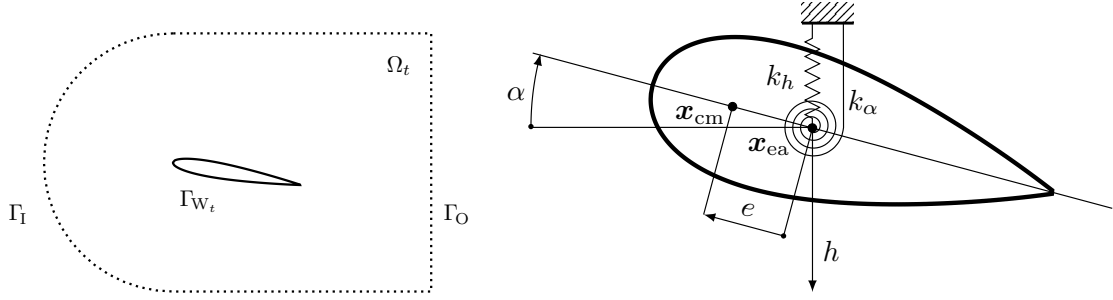
187

Figure 1: (Left) Sketch of the computational domain Ω_t. (Right) Sketch of the airfoil with two degrees of freedom. $\boldsymbol{x}_{\mathrm{cm}}$ and $\boldsymbol{x}_{\mathrm{ea}}$ denote position of the center of mass and the elastic axis, respectively with e being its relative distance, i.e., eccentricity.

for the turbulent kinetic energy k_T

$$\frac{1}{J}\frac{D^{\mathcal{A}}(Jk_T)}{Dt} + \mathrm{div}[k_T(\boldsymbol{v} - \boldsymbol{w})] = P_{k_T} + R_{BP} + R_{NAT} - \omega k_T - D_T +$$
$$+ \mathrm{div}\left[\left(\nu + \frac{\alpha_T}{\sigma_k}\right)\mathrm{grad}(k_T)\right], \quad (5)$$

and for the specific dissipation rate ω is given by

$$\frac{1}{J}\frac{D^{\mathcal{A}}(J\omega)}{Dt} + \mathrm{div}[\omega(\boldsymbol{v} - \boldsymbol{w})] = C_{w1}\frac{\omega}{k_T}P_{k_T} + \left(\frac{C_{wR}}{f_W} - 1\right)\frac{\omega}{k_T}(R_{BP} + R_{NAT}) -$$
$$- C_{w2}\omega^2 + C_{w3}f_\omega\alpha_T f_W^2\frac{\sqrt{k_T}}{d^3} + \mathrm{div}\left[\left(\nu + \frac{\alpha_T}{\sigma_\omega}\right)\mathrm{grad}(\omega)\right], \quad (6)$$

Here, the right hand side terms in equations (4) to (6) – e.g. P_{k_T}, R_{BP}, etc. – correspond to the notation used in [5]. The Reynolds stress (3) is calculated based on the solution of these equations with the aid of the quantities $k = k_T + k_L$, ω, see [5].

The flow model is coupled with the non-linear system of ordinary differential equations describing the motion of the rigid airfoil, see Figure 1. The motion of such an airfoil is described by the system of non-linear ordinary differential equations (see e.g. [7])

$$m\ddot{h} + k_h h + S_\alpha\ddot{\alpha}\cos\alpha - S_\alpha\dot{\alpha}^2\sin\alpha = -L(t),$$
$$S_\alpha\ddot{h}\cos\alpha + I_\alpha\ddot{\alpha} + k_\alpha\alpha = M(t),$$
$$(7)$$

where α is the rotation around the elastic axis (clockwise positive) and h denotes the vertical displacement of the elastic axis (downwards positive), see Figure 1, m is the mass of the airfoil, S_α is the static moment around the elastic axis, I_α is the inertia moment around the elastic axis, k_h is the bending stiffness, and k_α is the torsional stiffness. L and M denotes the aerodynamic lift force (upwards positive) and the

aerodynamic torsional moment (clockwise positive), respectively. The aerodynamic lift force L acting in the vertical direction and the torsional moment M are defined by

$$L = -l \int_{\Gamma_{W_t}} \sum_{j=1}^{2} (\mathsf{T}_{2j} + \mathsf{R}_{2j} - \rho p \delta_{2j}) n_j \, dS, \quad M = l \int_{\Gamma_{W_t}} \sum_{i,j=1}^{2} (\mathsf{T}_{ij} + \mathsf{R}_{ij} - \rho p \delta_{ij}) n_j r_i^{\mathrm{ort}} \, dS, \quad (8)$$

where $r_1^{\mathrm{ort}} = -(x_2 - x_2^{\mathrm{ea}})$, $r_2^{\mathrm{ort}} = x_1 - x_1^{\mathrm{ea}}$ and l is the depth of the airfoil section and $\boldsymbol{n} = (n_1, n_2)$ is the unit outer normal to $\partial\Omega_t$ on Γ_{W_t} (pointing into the airfoil).

The system of equations (1) is equipped with an initial conditions $\boldsymbol{v}(\boldsymbol{x}, 0) = \boldsymbol{v}_0(\boldsymbol{x})$, $p(\boldsymbol{x}, 0) = p_0(\boldsymbol{x})$ and by boundary conditions prescribed at $\partial\Omega_t = \Gamma_{\mathrm{I}} \cup \Gamma_{W_t} \cup \Gamma_{\mathrm{O}}$, see Figure 1. Velocity $\boldsymbol{v}_{\mathrm{I}}$ is prescribed at the inlet part of the boundary Γ_{I}, no-slip boundary condition, i.e., $\boldsymbol{v} = \boldsymbol{w}$, at the moving part of the boundary representing the surface of the airfoil Γ_{W_t} and $p = 0$ at the outlet part of the boundary Γ_{O}. Three equations of the turbulence model, i.e., (4), (5) and (6) are also equipped by an initial conditions $k_T(\boldsymbol{x}, 0) = k_{T0}(\boldsymbol{x})$, $k_L(\boldsymbol{x}, 0) = k_{L0}(\boldsymbol{x})$ and $\omega(\boldsymbol{x}, 0) = \omega_0(\boldsymbol{x})$ and by boundary conditions prescribed on $\partial\Omega_t$. The boundary conditions at the solid wall, i.e., at Γ_{W_t}, are $k_T = 0$, $k_L = 0$ and $\partial\omega/\partial n = 0$ (see e.g. [5], [11]). The values of k_T and ω at the inlet part Γ_I are set according to parameters of the inlet flow and $k_L = 0$. The system (7) is equipped with initial conditions prescribing the values $h(0)$, $\alpha(0)$, $\dot{h}(0)$, $\dot{\alpha}(0)$. The flow model, i.e, (1), (4), (5), (6), and structure model, i.e., (7), are coupled thought the aerodynamic lift force and the torsional moment (8).

3. Numerical method

The fluid flow solver is based on OpenFOAM's implementation of the finite volume method, see e.g. [8]. In order to resolve the incompressibility of the fluid the PIMPLE algorithm is used to approximate the fluid flow, see e.g. [4], [8]. Approximation of the ALE derivative is done by the second order backward difference formula, see e.g. [2], [8].

Pressure-velocity coupling. The velocity and the pressure are treated in a segregated approach, with the pressure field computed by a pressure correction equation that exploits the discrete momentum equation to replace the velocity field in the continuity equation with a pressure term. The PIMPLE algorithm can be summarized as: first, the momentum predictor step is performed, which corresponds to the finite volume discretization of the equation (1) to obtain new estimation of the velocity field. This velocity field is not in general divergence-free, to solve this problem the pressure correction equation is solved. Finally, the velocity is corrected with the new estimation of the pressure field. The PIMPLE algorithm is shown on Figure 2 (Left). Let us mention that, in the case of using the SIMPLE loop, an under-relaxation factors are used, see e.g. [4] or [8].
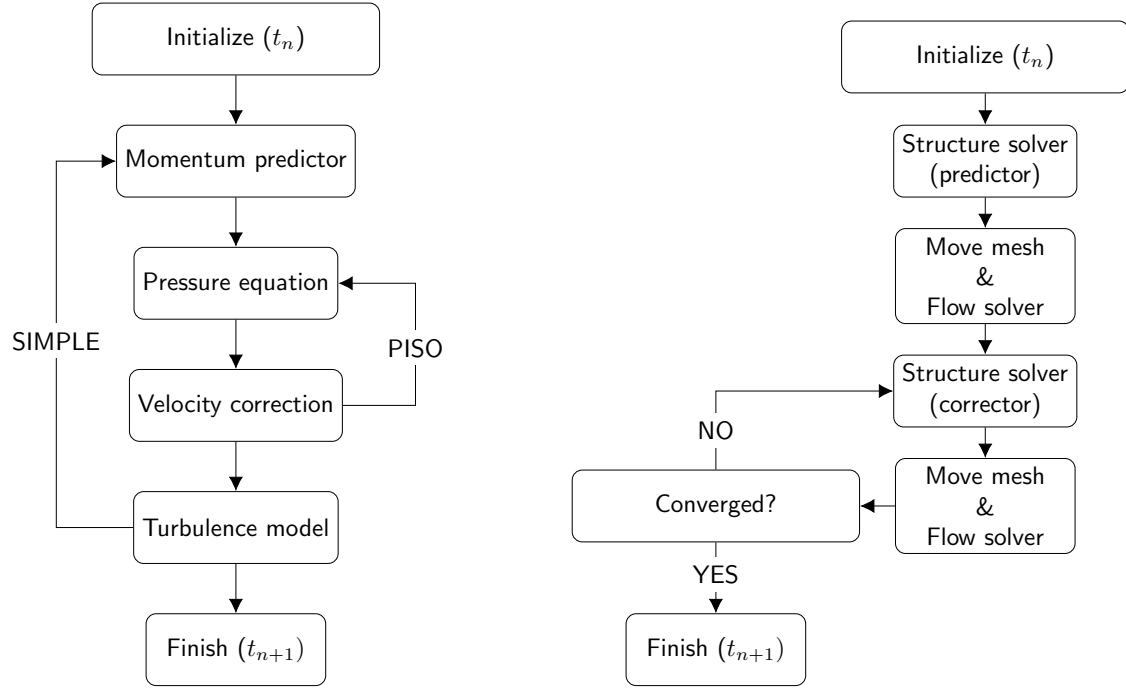
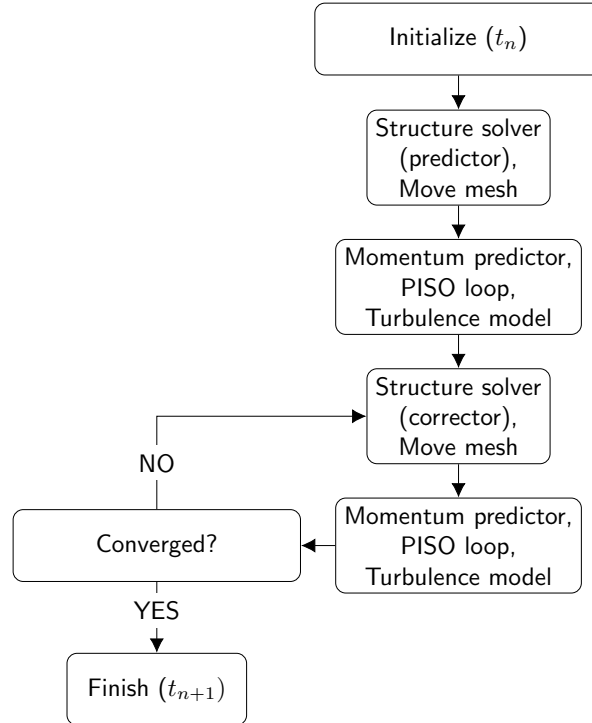Figure 2: (Left) Flowchart of the PIMPLE algorithm. (Right) Flowchart of the loose/strong coupling algorithms.

Figure 3: Flowchart of the combined strong coupling algorithm.

Coupling algorithms.   The system (7) is solved by second order Adams-Bashforth-Moulton predictor-corrector method, see e.g. [1]. Figure 2 (Right) shows flowchart of the loose/strong coupling algorithm with the convergence check being

$$r = \max_i \left[\frac{|(\dot{y}_i)_{k+1}^{n+1} - (\dot{y}_i)_k^{n+1}|}{|(\dot{y}_i)_{k+1}^{n+1}|} \right] < 10^{-4}, \quad \boldsymbol{y} = [\dot{h}, \dot{\alpha}], \tag{9}$$

where index k indicates number of convergence checks starting at $k = 0$. For $k = 0$, the algorithm is loose. Figure 3 shows flowchart of the combined strong coupling algorithm, which takes advantage of the iterative process of the fluid flow solver, i.e., SIMPLE loop.

4. Numerical results

In this section the numerical results of the coupled problem of the fluid flow and structure interaction is presented. The described methods were applied to the analysis of the flow induced vibrations of the profile NACA 0012 profile. The computation was carried out for the same data as in [10]: $m = 0.086622\,\text{kg}$, $S_\alpha = -0.000779673\,\text{kg m}$, $I_\alpha = 0.000487291\,\text{kg m}^2$, $k_h = 105.109\,\text{N m}^{-1}$, $k_\alpha = 3.695582\,\text{N m}$ rad^{-1}, $l = 0.05\,\text{m}$, $c = 0.3\,\text{m}$, $\rho = 1.225\,\text{kg m}^{-3}$, $\nu = 1.5 \cdot 10^{-5}\,\text{m s}^{-2}$ and the position of the elastic axis $x_1^{\text{ea}} = 0.4c = 0.12\,\text{m}$. The presented results are for far field flow velocities $U_\infty = 35, 40, 45\,\text{m s}^{-1}$, which yield the Reynolds numbers $\text{Re}_\text{c} = 700\,000, 800\,000, 900\,000$. The computation starts at time $t = 0$ with the initial condition being the fully developed flow with the airfoil in a fixed position given by the prescribed initial translation $h(0) = -50\,\text{mm}$ and the initial angle of attack $\alpha(0) = 6\,\text{deg}$. Initial velocities of the structural model are $\dot{h}(0) = 0$ and $\dot{\alpha}(0) = 0$. The results of the airfoil motion due to the fluid-structure interaction for time $t \in \langle 0, 1 \rangle$ are shown in Figures 4 for the far field velocities $U_\infty = 35, 40, 45\,\text{m s}^{-1}$. The results of the loose, strong and combined strong coupled algorithms are shown. Obtained results indicate the need of the use of the strong coupled algorithm in post flutter regimes (for this model the critical velocity is approximately $37\,\text{m s}^{-1}$). Furthermore, in our test case, the combined strong coupling algorithm proved to get very close solutions to the strong coupling algorithm with less computer-time needed, see Table 1.

5. Conclusion

In this paper the modification of the OpenFOAM's solver is presented, which allows solution of an aeroelastic problem with the transition to turbulence taken into account. The results show the need for the strong coupling algorithms in the post-flutter regime. Furthermore, by the combination of the PIMPLE and strong coupling algorithms significant reduce in computer-time needed for the simulation were observed for our test case.
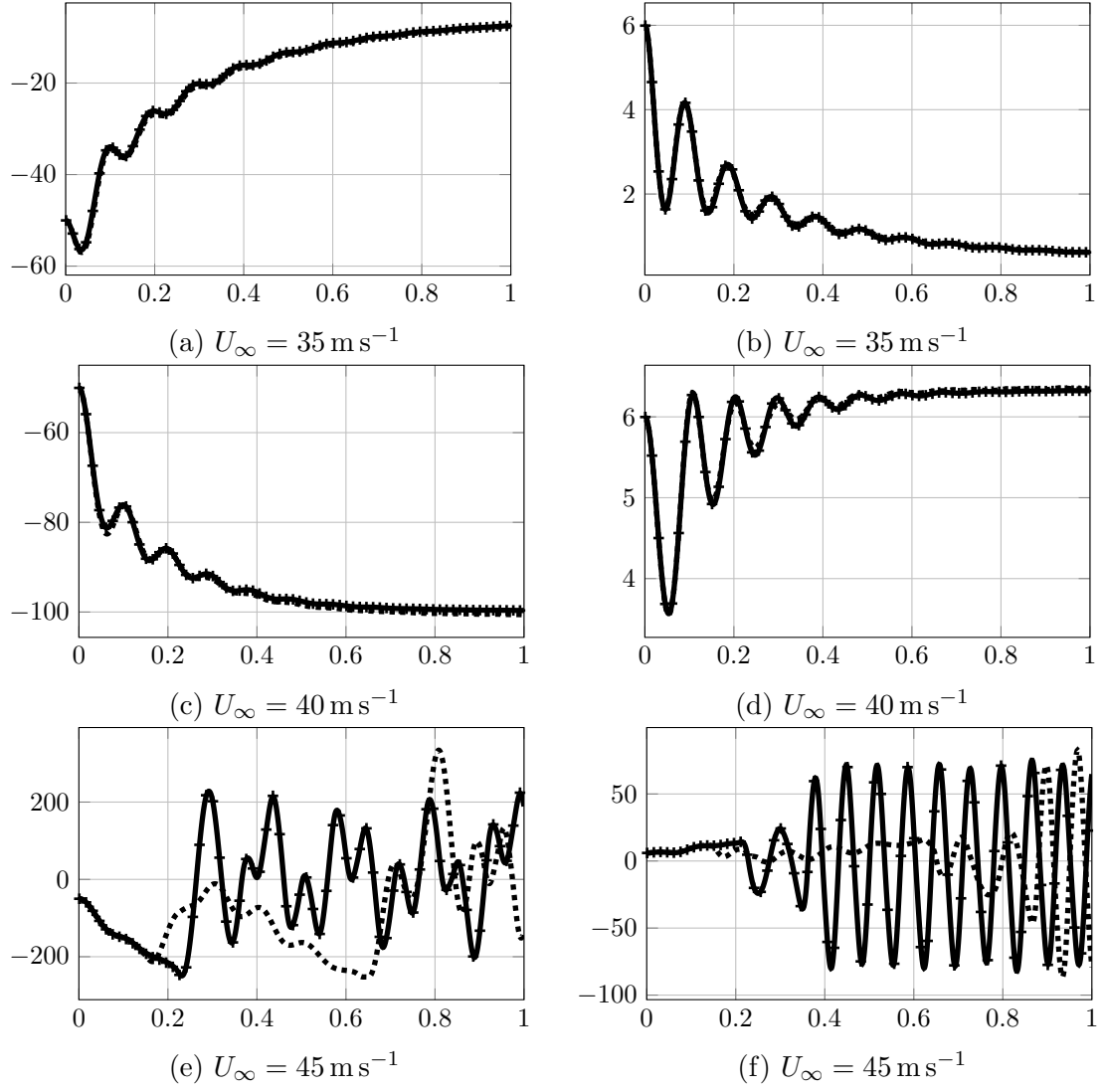
(a) $U_\infty = 35\,\mathrm{m\,s^{-1}}$

(b) $U_\infty = 35\,\mathrm{m\,s^{-1}}$

(c) $U_\infty = 40\,\mathrm{m\,s^{-1}}$

(d) $U_\infty = 40\,\mathrm{m\,s^{-1}}$

(e) $U_\infty = 45\,\mathrm{m\,s^{-1}}$

(f) $U_\infty = 45\,\mathrm{m\,s^{-1}}$

Figure 4: (Left) $h\,[\mathrm{mm}]$ and (Right) $\alpha\,[\mathrm{deg}]$. Dotted, dashed marked by $+$ and solid lines are graphs of the solutions of the loose, strong and combined strong coupling algorithms, respectively.

U_∞	Weak	Strong	Combined Strong
35	5	19.7	6.5
40	5	21.1	8.6
45	5	27.1	11.2

Table 1: Mean value of SIMPLE iterations per time-step during the computation for loose, strong and combined strong coupling algorithms for the far field velocity $U_\infty = 45\,\mathrm{m\,s^{-1}}$.

192

References

[1] Butcher, J.C.: *Numerical Methods for Ordinary Differential Equations*. Wiley, 2016, third edn.

[2] Demirdžić, I. and Perić, M.: Space Conservation Law in Finite Volume Calculations of Fluid Flow. International Journal for Numerical Methods in Fluids **8** (1988), 1037–1050.

[3] Feistauer, M., Horáček, J., Růžička, M., and Sváček, P.: Numerical Analysis of Flow-Induced Nonlinear Vibrations of an Airfoil with Three Degrees of Freedom. Computers & Fluids **49** (2011), 110–127.

[4] Ferziger, J.H. and Perić, M.: *Computational Methods for Fluid Dynamics*. Springer, 2002, third edn.

[5] Fürst, J., Příhoda, J., and Straka, P.: Numerical Simulation of Transitional Flows. Computing **95** (2013), 163–182.

[6] Habchi, C. et al.: Partitioned Solver for Strongly Coupled Fluid-Structure Interaction. Computers & Fluids **71** (2013), 306–319.

[7] Horáček, J. and Sváček, P.: Finite Element Simulation of a Gust Response of an Ultralight 2-DOF Airfoil. In: *Proceedings of the ASME 2014 Pressure Vessels & Piping Conference*. 2014 .

[8] Moukalled, F., Mangani, L., and Darwish, M.: *The Finite Volume Method in Computational Fluid Dynamics: An Advanced Introduction with OpenFOAM and Matlab*. Springer, 2016.

[9] Pope, S.B.: *Turbulent Flows*. Cambridge University Press, 2000.

[10] Sváček, P., Feistauer, M., and Horáček, J.: Numerical Simulation of Flow Induced Airfoil Vibrations with Large Amplitudes. Journal of Fluids and Structures **23** (2007), 391–411.

[11] Walters, D. and Cokljat, D.: A Three-Equation Eddy-Viscosity Model for Reynolds-Averaged Navier-Stokes Simulations of Transitional Flow. Journal of Fluids Engineering **130** (2008), 121 401–1–121 401–14.

[12] Weller, H.G., Tabor, G., Jasak, H., and Fureby, C.: A Tensorial Approach to Computational Continuum Mechanics Using Object-Oriented Techniques. Computers in Physics **12** (1998), 620–631.

[13] Winter, O. and Sváček, P.: Interaction of Incompressible Fluid Flow and a Vibrating Airfoil. AIP Conference Proceedings **1978** (2018). DOI: 10.1063/1.5043666.